Research on Engineering Structures & Materials
www.jresm.org
MIM Research Group

Research Article

Influence of micro-addition of lanthanum on grain characteristics, mechanical properties, and corrosion behavior of CuAlNiMnLa shape memory alloy

Samuel J. Aliyu[1,a], Timothy Adeniyi Adekanye[*1,b], Adeolu A. Adediran[1,2,c], Oluwasogo L. Ogundipe[1,d]

[1]*Department of Mechanical Engineering, Landmark University, Omu- Aran. Nigeria*
[2]*Department of Mechanical Engineering Science, University of Johannesburg, South Africa*

Article Info

Article history:

Received 10 July 2024
Accepted 22 Aug 2024

Keywords:

Copper-based alloys;
Surface morphology;
Grain characteristics;
Rare earth metal;
Mechanical properties;
Corrosion behavior

Abstract

The study investigated the grain size criteria, mechanical characteristics, and corrosion behavior of Cu-14Al-4.5Ni-0.7Mn shape memory alloy (SMA) with the micro-addition of 0.06 wt% Lanthanum (La). Using standard melting and casting procedures, the alloy compositions were melted at 1300 °C in an arc furnace with an argon atmosphere. The cast compositions without thermal treatment were machined and tested for physical properties including density and percentage porosity, corrosion behavior, and mechanical properties like hardness, ultimate tensile strength, yield strength, fracture strain, percentage elongation, specific strength, and fracture toughness. The average grain size, profile plot, and grain size distribution were all determined using ImageJ software. The microstructural observations revealed the presence of α-phase, β-phase, and intermetallic phases, including the coarse α+γ2 phase, which contributed to the improved characteristics. The inclusion of lanthanum resulted in a drop in the average grain size of the parent alloy from 9.25 µm to 6.08 µm, indicating a clear correlation between property improvement and microstructure refinement. The composition's tensile strength and yield strength increased with the La micro-addition by 22.14% and 20.31% respectively while the hardness value increased by 17.3%. The fracture strain of the modified composition increased by 20% compared to the unmodified composition while the percentage elongation increased by 7.7% and a 22.5% increase in fracture toughness was achieved. The modified CuAlNiMn SMA also showed a significant improvement in corrosion resistance to NaCl solutions which was so evident at 144 hours of the study for 0.5 M of NaCl solution and at 96 hours for 1.0 M of NaCl solution. The results showed that CuAlNiMn SMA with micro-addition of La had better physical, corrosion, and mechanical characteristics than unmodified CuAlNiMn alloys.

1. Introduction

Shape memory alloy (SMA) materials are advanced metallic materials that can revert to their original position after deformation when subjected to relevant thermal treatment. They have two distinct crystal structures: the higher-temperature Austenite structure and the lower-temperature Martensite structure [1]. A reversible austenite to martensite phase transformation is a prerequisite for the memory effect. Thermal (cooling and heating) or mechanical (loading) techniques can be used to achieve such phase transformation [2]. Shape memory alloys have been notably distinguished from other types of materials because of their pseudo-elasticity [3] and shape memory effect (SME) features [4]. In the biomedical and

*Corresponding author: adekanye.adeniyi@lmu.edu.ng
[a] orcid.org/0000-0002-5281-9494; [b] orcid.org/0000-0002-7581-8785; [c] orcid.org/0000-0001-9457-1071; [d]orcid.org/0009-0001-4630-2253
DOI: http://dx.doi.org/10.17515/resm2024.347me0710rs

engineering industries, SMAs have been reported in various research as the main components in products like thermal actuators [5], pumps, linear engines [6], separators, automated arms [7], hydraulic tube couplings [8], lens frames, and electrical system breakers [9].

Shape memory alloys are categorized according to the alloying elements. We can differentiate between alloys based on Nickel (such as; Ni-Ti, Ni-Mn-Ga), Copper (such as; Cu-Zn-Al, Cu-Al-Ni), Iron (such as; Fe-Mn, Fe-Mn-Si), Rare metals (such as; Au-Cd, Au-Ag, Pt-Al), etc. depending on this base material [10]. They are regarded as the SMA systems with the most potential for both functionality and commerce. For technological and industrial applications, Cu-based SMAs are widely recognized as the most affordable and processing-sustainable SMA systems. The primary benefit of Cu-based SMAs over other SMAs is specifically their economic effect (affordable cost) [11]. Specifically, Cu-Al-Ni alloys have applications in a variety of industrial domains, particularly where elevated transformation temperatures (up to 200 °C) are necessary [10]. High transformation temperatures, strong corrosion resistance, high resistance to functional property deterioration during aging processes, and a fair price all influence the choice of this class of alloys for application. They have a significant strain recovery (about 5%), which is second only to the NiTi systems (about 8%) [12], and they may be processed by conventional casting methods [13]. In light of this, Cu-based SMAs are now well-regarded when it comes to applications in electrical and thermo-responsive industrial [14], technological systems and biomedical industries [15].

As a consequence of the high elastic anisotropy of the parent β phase, large grain size, brittle Ɣ2 (Cu_9Al_4) phase, and formation of stress-induced martensites along grain boundaries upon quenching equiaxed polycrystalline CuAlNi alloy is prone to intergranular fracture during plastic deformation [16] and lack of cold-working ability due to high brittleness [17], which has been reported to have limited the alloy's engineering applications [18]. A potential remedy to this challenge is the addition of suitable rare metals (refining elements) such as Ce, La, Co, B, and Ti, which form the precipitates that restrict the size and growth of the grains. Moreover, the rapid-solidification technique or powder metallurgy used in the alloy's production is very effective in achieving a fine-grain microstructure of SMA. Grain modification and texture control are two significant methods used to improve the mechanical properties of the polycrystalline CuAlNi alloy. These two techniques are crucial in relieving the concentration of stress at grain boundaries, which in turn prevents fractures between granular layers and increases the alloy's flexibility [19]. By partially substituting the aluminum component, Manganese is introduced as an alloying element to the CuAlNi alloy to improve its ductility and stability. Additionally, it permits the betatising process to be carried out at lower temperatures and expands the β phase's stable domain [20]. In addition, Manganese is added to improve thermoelastic and pseudoelastic performance [21] and Saud et al. [22] reported that the inclusion of Manganese also lowers the rate of corrosion.

This research aimed to investigate the effect of micro-addition of La as a rare metal on the CuAlNiMn SMA in its as-cast condition through casting techniques. The findings provide information on the porosity, hardness, tensile, specific strength, fracture toughness, and corrosion behavior of the CuAlNiMn SMA system.

2. Materials and Method

2.1. Materials

To produce the Cu-Al-Ni-Mn base composition for shape memory alloys, pure-grade billets of copper, nickel, manganese, and aluminum were used as the base materials. Analytical high-quality lanthanum (La) powder was chosen to be the microalloying additive. The components for Cu, Al, Ni, Mn, and La were purchased from authorized local suppliers.

2.2. Method

2.2.1. Alloy Design and Production

Cu-14%Al-4.5%Ni-0.7%Mn and Cu-14%Al-4.5%Ni-0.7%Mn-0.06La were the two components that piqued curiosity in this study. The study followed Alaneme et al.'s approach in adopting charge computations and alloy production methods to reach these alloy compositions [23]. The alloy compositions were developed in an arc furnace with an argon atmosphere using standard melting and casting procedures. The melts were then poured into cylinder-shaped cast iron metal molds that measured 200 mm in length and 20 mm in diameter using 1300 °C temperature as the heat index. The cast specimens were taken out, fettled, and then machined into different test specimens for microstructural, mechanical, and corrosion examination. Table 1 displays the chemical compositions of the alloys developed and the matching sample designations.

Table 1. Composition of the CuAlNiMn SMA, both unmodified and modified with La

Compositions	Cu	Al	Ni	Mn	La
C 1	80.80	14	4.5	0.7	-
C 2	80.75	14	4.5	0.7	0.06

2.2.2. Microstructural Characterization

The CuAlNiMn alloys that were produced, both modified and unmodified, had their microstructures observed under an optical microscope (Model: L2003A). The sample's surfaces were polished to a mirror-like metallographic finish by a series of grinding operations using abrasive papers with grit sizes of 220, 500, 1000, and 1200. Etching was done with a solution of 2.5 g $FeCl_3$, 10 mL HCl, and 48 mL ethanol. The grain analysis, comprising the estimation of average grain size (using Eq 1), profile plot, and grain size distribution, was accomplished with the support of ImageJ software (using the simple linear intercept approach) adopting the method outlined by Peregrina-Barreto et al [24].

$$Average\ Grain\ Size = \frac{Line\ Length}{Number\ of\ Grains} \tag{1}$$

2.2.3. Measurement of Density and Porosity in Percentage

Density measurements were used to estimate the compositions' levels of porosity. This was accomplished by analyzing the theoretical and experimental densities of every composition. An Ohaus Pioneer digital weighing balance (Model: PA214) with a high-precision tolerance of 0.0001g was used to weigh the test samples to determine the experimental density of the samples. In every instance, the measured weight was divided by the volume of the corresponding samples. The rule of mixture as stated in Eq (2), was used for the computation of the theoretical density.

$$\rho_C = \sum V_E * \rho_E \tag{2}$$

Where $\boldsymbol{\rho_C}$ is the density of the composition; $\mathbf{V_E}$ is the volume fraction of the element ;

$\boldsymbol{\rho_E}$ is the density of the element. Using the relations stated in Eq (3), the percent porosity of the composites was determined.

$$\%\ Porosity = \left(\frac{\rho_T - \rho_{EX}}{\rho_T}\right) \times 100 \tag{3}$$

Where, ρ_T *is the Theoretical Density* $\left(\frac{g}{cm^3}\right)$; ρ_{EX} *is the Experimental Density* (g/cm^3)

2.2.4. Mechanical Characterization

- Hardness Testing

The Emcotest Durascan Microhardness Tester was equipped with the cutting-edge application ecos Workflow, was utilized to assess the hardness of the Cu-Al-Ni-Mn-based alloys that were produced. The samples were prepared using a finely finished cylindrical flat surface, and the ASTM E92–23 standard was followed during the testing process [25]. A 100g load was used for the hardness test, with a 10-second dwell period. The hardness indentation was performed at least five times, and the average hardness values were determined.

- Tensile Test

A universal testing device (Instron model 3369) was utilized to perform tensile testing on the as-cast CuAlNiMn SMA. The test samples were machined following the tensile test standards, measuring 30 mm in length of the gauge and 5 mm in diameter. Samples were mounted on the testing platform, the test samples were drawn under tension with a strain rate of 10^{-3}/s until they fractured. The ASTM E8/E8M-22 criteria were followed during the preparation of samples, evaluation, and data analysis [26]. For every composition of CuAlNiMn SMA produced, three repeatable tests were carried out to ensure the test results' dependability and repeatability.

- Fracture Toughness

The fracture toughness values of the CuAlNiMn SMA were evaluated by using the circumferential notch tensile (CNT) testing method as reported by Alaneme [23] and Alaneme & Umar [27]. The CuAlNiMn SMA compositions were shaped to precisely measure the 30 mm gauge length, 6 mm gauge diameter (D), 4.5 mm notch diameter (d), and 60° of the notch angle to conduct the evaluation. A standardized testing device with a strain rate of 10^{-3}/s was used to bend the samples until they broke while they were in the stage of testing. The relation was used to determine the fracture loads (Pf) obtained from the load-extension data of the alloys to evaluate their fracture toughness using Eq (4) as stated by [27].

$$K_{1c} = \frac{p_f}{D^{3/2}} \left[1.72 \left(\frac{D}{d}\right) - 1.27\right] \tag{4}$$

Where the specimen diameter (D) and the notched section diameter (d) are the corresponding values. By using the relationships described in Eq (5) [27], the values for the fracture toughness were obtained for validation under plane strain conditions.

$$D \geq \left(\frac{K_{1c}}{\sigma_y}\right)^2 \tag{5}$$

For every composition of CuAlNiMn SMA, three tests were rerun to make sure the results were dependable and accurate.

2.2.5. Corrosion Test

The following materials, instruments, and reagents were employed in the study following Edoziuno et al [28]: 500-milliliter beakers, 100-milliliter volumetric flasks, emery paper, distilled water, 0.5 M and 1.0 M sodium chloride (NaCl) solutions made with laboratory-quality materials, filter paper, and dry clothes, analytical grade acetone substance including unmodified and modified CuAlNiMn SMA specimens in the form of cylindrical 20 mm diameter by 10 mm length are all included.

Before any further processing, the alloy specimens were cleaned and polished using emery papers of different sizes (such as 400, 800, and 1,200 grit), filter paper, and dry clothes. They were rinsed with distilled water from the faucet and thoroughly cleaned using acetone. Following a thorough air-drying process, the samples were weighed to four decimal places

(0.0001) on an analytical scale. After the samples were weighed, they were immersed in the measured NaCl concentrations. At 48-hour intervals (up to 240 hours), the compositions were removed from the test solutions and immediately given a quick washing with distilled water. Finally, an analytical scale was used to weigh the specimens, and the variations in weight at each period were recorded. Each sample's weight loss (mg) and corrosion rate (mm/yr) were assessed using ASTM G31-21 guidelines [29].

3. Results and Discussion

3.1 Microstructure Analysis, Grain Size Distribution, and Average Grain Size

CuAlNiMn and CuAlNiMn modified with 0.06 weight percent La alloying additions are shown in their as-cast microstructures in Fig. 1(a-b). The distribution of grain sizes in the CuAlNiMn and CuAlNiMn0.06La alloy systems is presented in Fig. 2. Based on the microstructures of the parent alloy shown in Fig. 1a, the structures composed of α-phase, β-phase, and a huge coarse intermetallic compound called α+γ2. The grains are coarse and dendritic, evenly distributed, but with an overabundance of undissolved copper. As illustrated in Fig. 1a, the composition alloy's microstructure revealed more of an undissolved Cu-alloy complex (dendritic grain) with an average grain size of 9.25 µm, which gave rise to the hard and brittle eutectoid α+γ2 phase which is the predominant phase [11,30]. This resulted in the low performance of mechanical properties displayed by the composition (CuAlNiMn). In contrast, Fig. 1b shows a notable increase in the number of rosette-shaped β-phase grains that were uniformly distributed throughout the α-phase, indicating full wettability of the grains and improved mechanical properties displayed by the CuAlNiMn–0.06%La alloy. Additionally, it was noted that the micro-addition of La to the concentration of the parent alloy system (CuAlNiMn) resulted in a reduction of the huge coarse grains (α+γ2 phase), indicating the soluble nature of elements in the copper matrix. The enhanced mechanical features exhibited by the alloy can be attributed to the size and dispersion of its grain [31].

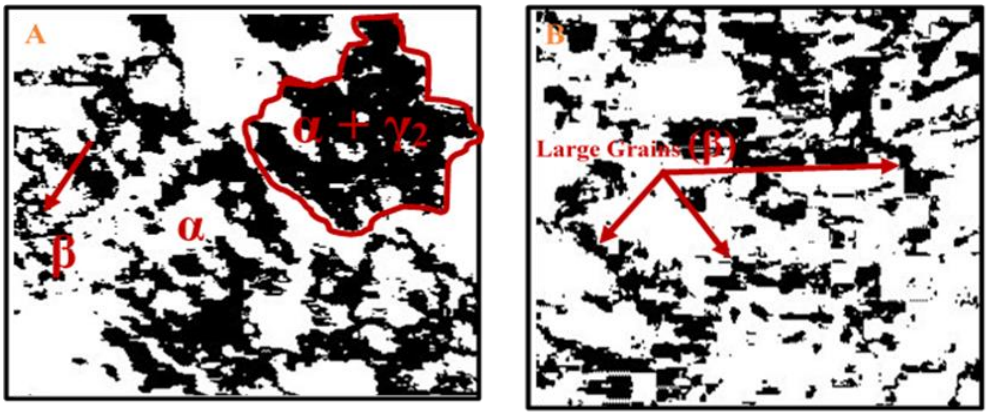

Fig. 1. Representative Optical Micrograph of as-cast structure for (a) CuAlNiMn and (b) CuAlNiMnLa

When 0.06 wt.% La was added to the parent alloy system (CuAlNiMn), a decrease in grain size was observed with a decrease in the solid solution region (Figure 1), which improved the mechanical properties. The average grain size of the parent alloy decreased from 9.25 µm to 6.08 µm after being doped, as shown in Fig. 2(a-b). As evident in Fig. 2, the strength and hardness of the Cu-14Al-4.5Ni-0.7Mn-0.06La alloy system increased by about 28.44 % and 10.77 %, respectively, as compared to the parent alloy. It is noted that the micro-addition of La

caused the average grain size to reduce drastically from 9.25 µm to 6.08 µm. Evidently, Fig. 2b showed a superior grain size distribution than the composition of the parent alloy.

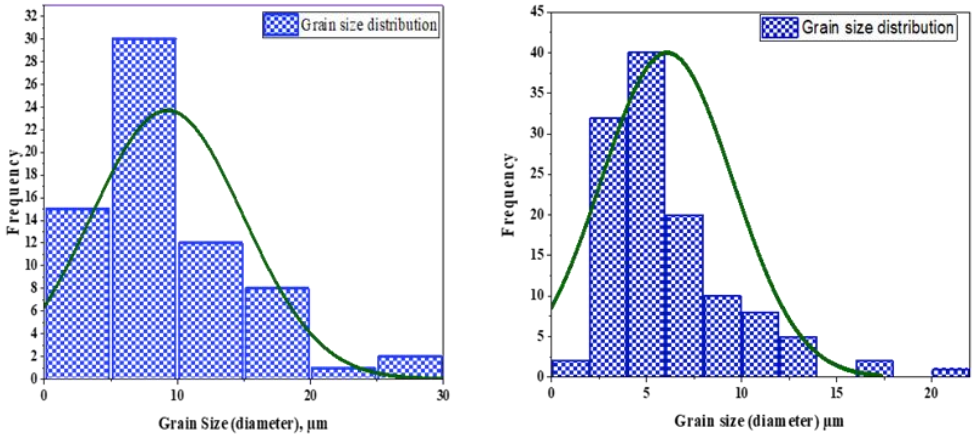

(a) (b)

Fig. 2. Grain size distribution of (a) CuAlNiMn (b) CuAlNiMnLa

3.2 Measurement of Density and Porosity

Table 2 displays the result of the percent porosity and density measurements of the CuAlNiMn SMA system. Comparing the two compositions, it is shown that the modified CuAlNiMn (C2) had lower porosity levels than the unmodified CuAlNiMn (C1) SMA system.

Table 2. The percentage porosity for the produced CuAlNiMn SMA

Composition	Theoretical density, (gcm^{-3})	Experimental density, (gcm^{-3})	Porosity (%)
C1	8.05323	7.963	1.12
C2	8.05162	7.963	1.10

It is observed that the micro-addition of the La causes the composites' percentage porosity to decrease. This shows that rare earth elements contribute to the excellence of the SMA produced by decreasing the percentage porosity. Additionally, the dispersion of La particles in the CuAlNiMn SMA was improved by the procedure, because the maximum permissible porosity value in sand casting composition is less than 4% [32], for porosity has a significant impact on material behavior.

3.3 Mechanical Characteristics

3.3.1 Hardness Properties

Figure 3 shows the variation in the CuAlNiMn SMA hardness with and without the micro-addition of La. The inclusion of La was found to marginally boost the alloys' hardness; in comparison to the unaltered CuAlNiMn, the weight percentage of La increased the composition's hardness value by 17.3%. The inclusion of La as a micro-alloying addition is responsible for the increased hardness found in the modified CuAlNiMn SMA. This change in grain edge morphology and reduction of elongated grain width (i.e., grain thickness) were the outcomes of these additions [33]. A hardening effect caused by the finely dispersed particles

could account for the modified CuAlNiMn SMA's increased hardness value [34]. The Hall-Petch relation is supported by the enhanced resistance to indentation with smaller grain sizes [35].

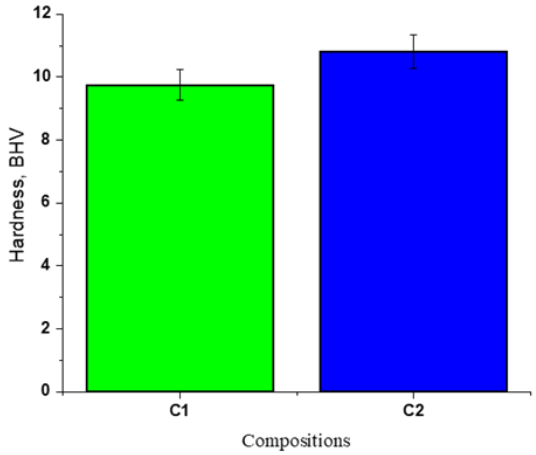

Fig. 3. Variation in hardness value of the produced composition

3.3.2. Tensile Properties

The ultimate tensile and yield strength are shown in Fig. 4. As observed, the tensile strength and yield strength of the composition increase with the micro-addition of La by 22.14% and 20.31% respectively. However, it was observed that the ultimate tensile and yield strengths for unmodified alloys were lower compared with the La-modified CuAlNiMn SMA. Hence, it is noteworthy that the inclusion of rare earth elements significantly improved the strength of the composition. The Rare earth elements help in achieving a refined and homogeneous structure by removing voids and micro-voids and also help in redistributing the particulates and second-phase particles resulting in considerable elimination of particle clusters and segregation. The elimination of a considerable number of voids and porosity in the composition strengthens its ability by lowering the possibility of particle separation under tensile loading [36,37].

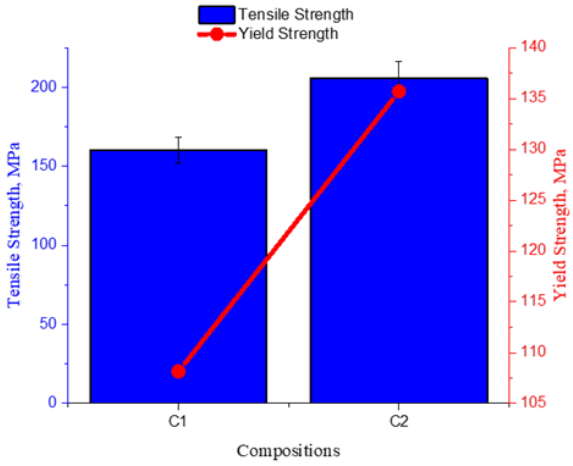

Fig. 4. Ultimate tensile strength and yield strength of the compositions

3.3.3 Fracture Strain Properties

The fracture strain for the compositions is shown in Fig. 5. It is noted that there was an increase in the fracture strain owing to the addition of La compared with the unmodified CuAlNiMn SMA. Sample C2 has the greatest strain improvement with a 20 % increase compared with C1. This shows the possibility of the CuAlNiMn system to withstand plastic deformation and therefore the rare earth metals modification improves their cold workability especially when the alloy is solution heat-treated [38,39].

3.3.4 Percentage Elongation Properties

Figure 5 shows the percentage elongation of the produced compositions. The highest percentage elongation was observed in sample C2 (0.06 wt % of La addition) with a 7.7 % increase when compared with the unmodified CuANiMn alloy. This is due to the ability to achieve better interphase interaction between the CuAlNiMn SMA particles and the rare earth metals.

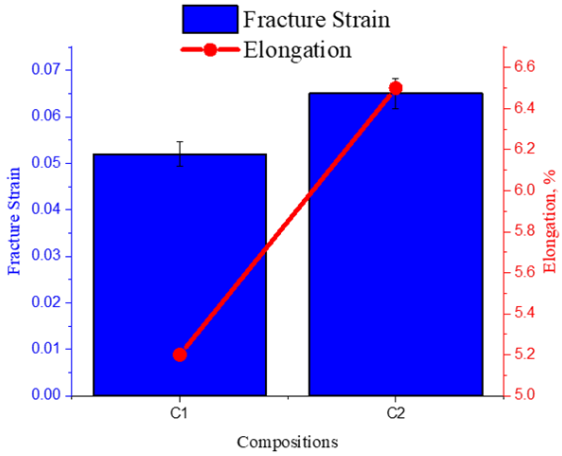

Fig. 5. Variation of fracture strain and percentage elongation of the produced compositions

It is worth noting that rare metals are naturally ductile compared to the brittle CuAlNiMn system [22,40,41]. It implies that the CuAlNiMn SMA enhanced with La will have a greater ability to withstand plastic deformation. The reduction in percentage elongation of unmodified CuAlNiMn alloy can be ascribed to its sharp end grain boundaries, which can limit deformation through plasticity because of the triaxial stress condition that is formed at these locations [23].

3.3.5 Specific Strength Properties

Specific strength, commonly referred to as a material's strengths-to-weight ratio, is an indication of a substance's durability. It is noted from Fig. 6 that the micro-addition of La increases the specific strength of the composition. C2 which has 0.06 wt% of La has the highest specific strength, compared to C1 which is an unmodified alloy, this is a result of the relatively higher density of the composition as shown in Table 2. This implies that grain structures with thinner walls of higher material strength-to-weight ratio can be produced using La as an additive to CuAlNiMn SMA without any adverse effect on strength performance [42,43].

3.3.6 Fracture Toughness Properties

Figure 6 shows the evaluation of the fracture toughness for the CuAlNiMn SMA. The stated values are valid for fracture toughness, as condition, $D \geq (\frac{K_{1c}}{\sigma_y})^2$, given for the requirements for planar strain for the cylindrical round sample geometry were satisfied [27]. The micro-addition of La is noted to increase the fracture toughness of the CuAlNiMn SMA. 22.5% increase in fracture toughness was achieved for C2 with La addition. The inclusion of the rare metal in the alloy composition enhances the ability of the CuAlNiMn SMA to prevent the propagation of cracks. This is because the addition of La to CuAlNiMn SMA causes a stabilizing and refining impact on the grain, enhancing the alloy's toughness and resistance to the propagation of crack [39]. This means that in an application where impact absorption and resistance to fracture are essential service requirements, the CuAlNiMn SMA with La will be more dependable [42].

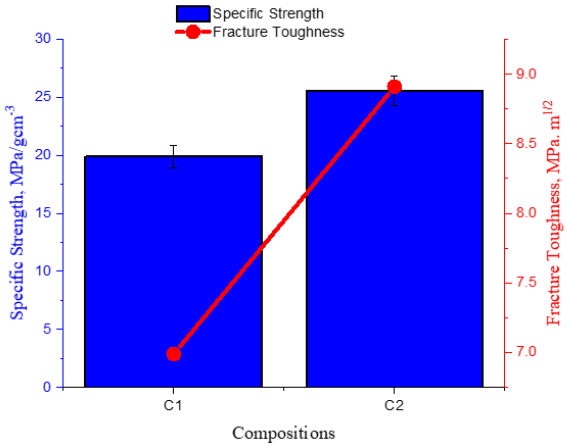

Fig. 6. Variation of specific strength and fracture toughness of the produced compositions

3.4 Corrosion Behavior

The variation of weight loss (mg) and corrosion penetration rate (mm/yr.) of the CuAlNiMn SMA in 0.5 M NaCl and 1.0 M NaCl solutions are presented in Fig. 7 and Fig. 8 respectively. Fig. 7(a), shows that the weight losses of the two alloy systems produced were less than 9 mg in the NaCl solution after 240 hours of experiment. The micro-addition of La has a modest effect on the alloy's resistance to corrosion in the solution, as may be seen by careful observation. Compared to the unmodified composition (C1) the corrosion tendency of the alloy was slightly reduced with the addition of the rare element. Fig 7(b) shows the weight loss variation in 1.0 M NaCl solution. It was noted that the weight losses of the compositions were less than 10.0 mg in the NaCl solution after 240 hours of experiment. The compositions are influenced by the addition of La rare earth metal, which results in a considerable weight decrease compared to the unmodified alloy (C1), which exhibits the greatest weight loss throughout the experiment. Figure 8 shows the corrosion penetration rate of the produced compositions in 0.5 M and 1.0 M of NaCl solutions. It was observed that the corrosion rate of the La-modified composition was reduced compared with the unmodified composition. It was also observed in Fig. 8(a) and 8(b) that C2 showed a resistance to corrosion (lowest corrosion penetrated rate) throughout the study while it was so evident at 114 hours for 0.5 M of NaCl solution and 96 hours for 1.0 M of NaCl solutions. In Fig. 7 and 8, it is observed that the addition of La to the CuAlNiMn SMA resulted in a significant improvement of the corrosion resistance of the CuAlNiMn SMA in NaCl solution.

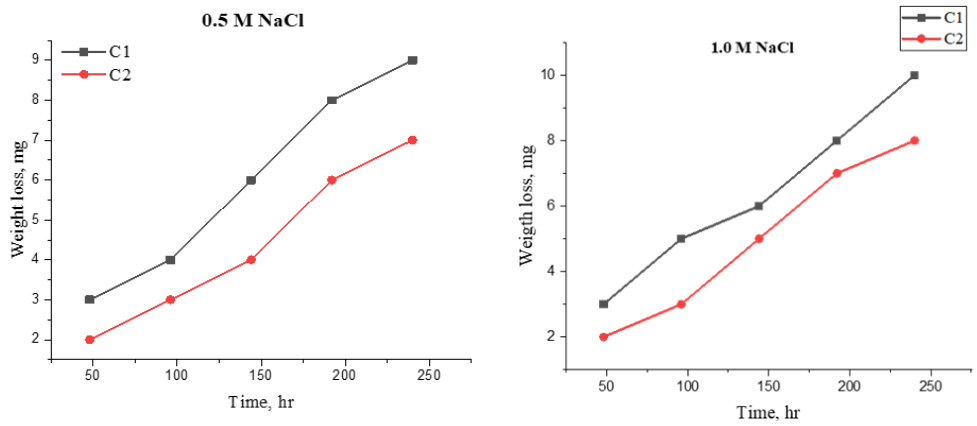

(a) (b)

Fig. 7. (a) Variation of weight loss for the produced CuAlNiMn-based SMA immersed in 0.5M NaCl solution, (b) Variation of weight loss for the produced CuAlNiMn-based SMA immersed in 1.0M NaCl solution

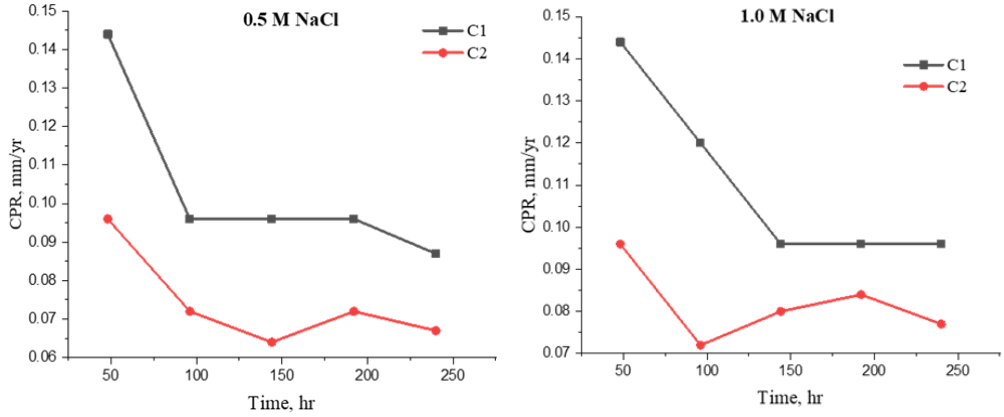

(a) (b)

Fig. 8. (a) Variation of Corrosion Penetration Rate for the produced CuAlNiMn-based SMA immersed in 0.5 M NaCl solution, (b) Variation of Corrosion Penetration Rate for the produced CuAlNiMn-based SMA immersed in 1.0 M NaCl solution

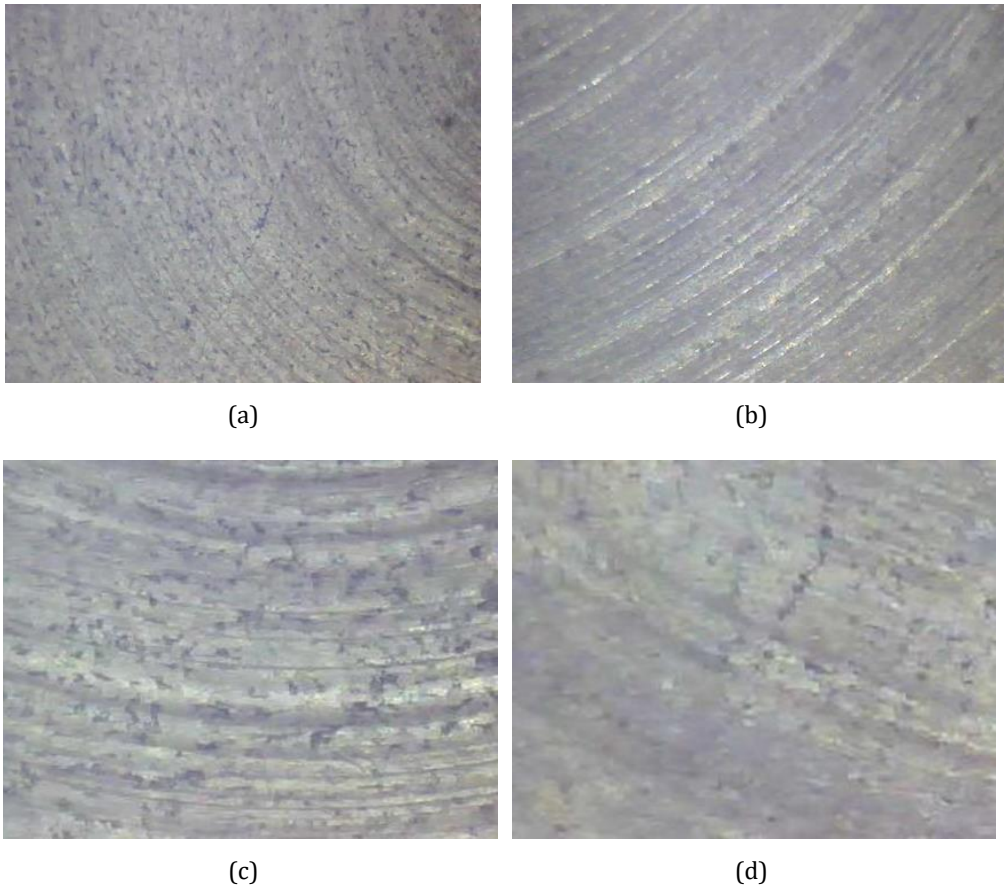

Fig. 9. Optical Microscope images of the samples with corroded surfaces; (a) C1 of 0.5 M of NaCl solution, (b) C2 of 0.5 M of NaCl solution, (c) C1 of 1.0 M of NaCl solution, and (d) C2 of 1.0 M of NaCl solution

After the corrosion test, the surfaces were subjected to an ultrasonic treatment in deionized water, dried in a desiccator, and then evaluated under an optical microscope at a magnification of 10 to ascertain the surface state, as illustrated in Fig. 9. Pits are evident on the surfaces of C1 and C2 as shown in Fig. 9a and 9b, which show a 0.5 M NaCl solution, but the surface of C2 shows less pitting corrosion. Also, both C1 and C2 of the 1.0 M NaCl solution in Fig. 9c and 9d follow the same pattern as Fig. 9a and 9b but there is more evidence of pitting corrosion compared to Fig. 9a and 9b due to the higher concentration of NaCl in the solution. This is a positive indicator that micro-additions of La into CuAlNiMn alloy can improve the corrosion resistance for applications in environments with moderate NaCl concentrations

4. Research Significance

Rare metals can greatly improve the performance of copper-based shape memory alloys (SMAs), providing several benefits for both basic science and practical applications. La metal addition to CuAlNiMn system is an active field of study with broad implications for applied engineering. It results in improved mechanical properties, increased resistance to corrosion, and the possibility of new, cutting-edge applications. This study attempts in developing a high-performance material suited for harsh environment.

5. Knowledge Gaps

Rare earth metals have been employed by several authors in their SMA research, it has been discovered that these metals are limited in availability in Cu-based SMAs. The influence of Lanthanum as an enhancer for improved grain characteristics, mechanical, and corrosion properties of CuAlNiMn shape memory alloy in its as-cast state have been examined in this study. Although the as-cast condition is the main emphasis, these alloys may be optimized by investigating various benefits and constraints in the solution treatments. Furthermore, alternative metal-forming processes (such as powder metallurgy and rapid solidification) and their effects on the inclusion and dispersion of rare metals in Cu-based SMAs have not been well explored. This requires a grasp of how processing factors influence the final properties of the alloy's system.

6. Nomenclature

SMA – Shape Memory Alloy
SME – Shape Memory Effect
C1 – Composition 1
C2 – Composition 2
Cu - Copper
Al – Aluminum
Ni – Nickel
Mn – Manganese
La – Lanthanum
Ce – Cerium
Ti – Titanium
Ga – Gallium
Zn – Zinc
Fe – Iron
Si – Silicon
Au – Gold
Ag – Silver
Cd – Cadmium
Pt – Platinum
Co – Cobalt
$FeCl_3$ – Iron (III) Chloride
HCl – Hydrochloric Acid
NaCl – Sodium Chloride
CPR – Corrosion Penetration Rate
ρ_C = Density of the composition
ρ_E = Density of the element
V_E = Volume fraction of the element
$\sum$ = Summation
ρ_T = Theoretical density
ρ_{EX} = Experimental density
CNT = Circumferential notch tensile
K_{1c} = Fracture toughness
p_f = Fracture load
D = Guage diameter
d = Notch diameter

7. Comparison of Previous Studies with The Current Study

It is evident from Table 3, that the inclusion of rare elements in the Cu-based SMA affects its properties. These elements produced a shape memory alloy system with a refined grain structure and could control the amount of austenite to martensite transition [47]. More study is necessary to fully understand the potential of La addition to Cu-based SMA since the effect has not been well studied.

Table 3. Comparative table showing the properties' results of the previous studies on Cu-based SMA and the current study with additions of rare metals

Reference(s)	Shape Memory Alloy (SMA)	Hardness (HV)	Strength (MPa)	Strain (%)	Porosity (%)	Corrosion Rate (mm/yr.)
[45]	CuAlNi	223.6	270	1.65	-	-
	CuAlNi0.97wt%Mn	225.4	450	3	-	-
	CuAlNi0.99wt%Ti	236.4	680	2.8	-	-
	CuAlNi1.14wt% Co	345	650	7	-	-

[46]	Cu11Al5Mn0.7Ti	190	266.5	0.65	-	-
	Cu11Al5Mn0.7Ti1Ta	233.5	386.1	1.05	-	-
	Cu11Al5Mn0.7Ti2Ta	247.2	393.6	1.22	-	-
	Cu11Al5Mn0.7Ti3Ta	211.9	357.4	0.98	-	-
[47]	Cu-14Al-4.5Ni	-	622	12.66	-	-
	Cu-14Al-4.5Ni-0.3Ce	-	659	16.45	-	-
	Cu-14Al-4.5Ni-1Ce	-	637	15.35	-	-
	Cu-14Al-4.5Ni-3Ce	-	340	6.99	-	-
[48]	Cu-11.9Al-2.5Mn	-	380	3.5	-	-
	Cu-11.9Al-2.5Mn-0.4CuZr	-	540	4.3	-	-
	Cu-11.9Al-2.5Mn-0.5CuZr	-	530	7.0	-	-
	Cu-11.9Al-2.5Mn-0.7CuZr	-	545	7.2	-	-
	Cu-11.9Al-2.5Mn-0.9CuZr	-	720	8.5	-	-
	Cu-11.9Al-2.5Mn-1.0CuZr	-	450	3.7	-	-
[49]	$(Cu83Al12Mn5)_{100}$ Ce_0	-	600	11	-	-
	$(Cu83Al12Mn5)_{99.5}$ $Ce_{0.05}$	-	890	15	-	-
$(Cu83Al12Mn5)_{1-x}$ Ce_x	$(Cu83Al12Mn5)_{99.90}$ $Ce_{0.1}$	-	800	16.7	-	-
	$(Cu83Al12Mn5)_{99.85}$ $Ce_{0.15}$	-	790	20.5	-	-
[50]	Cu-12.5Al-4Ni	-	-	-	12.96	2.68
	Cu-12.5Al-4Ni-1Ta	-	-	-	9.0	1.79
	Cu-12.5Al-4Ni-2Ta	-	-	-	7.5	0.74
	Cu-12.5Al-4Ni-3Ta	-	-	-	11.0	0.29
Current Study	Cu-14Al-4.5Ni-0.7Mn	9.75	160.21	5.2	1.12	0.087
	Cu-14Al-4.5Ni-0.7Mn-0.06La	10.8	205.77	6.5	1.10	0.067

8. Conclusions

CuAlNiMn alloy containing Lanthanum micro-alloying element has its mechanical properties, corrosion behavior, and grain characteristics adequately studied. The detailed outcomes of the present study are as follows:

- The microstructures and grain features directly affect the remarkable increase in mechanical properties that alloyed CuAlNiMn alloy demonstrates. The microstructure was composed of combinations of Cu-rich α-phase, β-phase with a substantial volume portion, and a huge coarse intermetallic compound called α+γ2.
- Adding La to the CuAlNiMn alloy caused a notable increase in the alloy's characteristics through grain refining. Following the micro-addition of the alloying element, the parent alloy's average grain size reduced from 9.25 μm to 6.08 μm, resulting in improved mechanical characteristics.

- The CuAlNiMn alloy without alloying elements performed the least favorably in terms of physical properties, with 1.12% porosity, and mechanical properties, with 9.75 BHV of hardness, 160.21 MPa of UTS, 108.15 MPa of yield strength, 0.052 of fracture strain, 5.2% of elongation, 19.89 MPa/gcm^3 of specific strength, and 6.99 MPa.m$^{1/2}$ of fracture toughness. In contrast, the CuAlNiMnLa alloy system achieved a lower percentage of porosity, higher value of hardness, UTS, yield strength, fracture strain, %elongation, specific strength, and fracture strain, with values of 1.10%, 10.80 BHV, 205.77 MPa, 135.71 MPa, 0.065, 6.5%, 25.57 MPa/gcm^3, and 8.91 MPa.m$^{1/2}$, respectively.
- Within the chosen media (0.5 M and 1.0 M of NaCl solutions), it was noticed from the corrosion rate and weight loss plots that the developed modified CuAlNiMn SMA exhibited a notable increase in corrosion resistance.
- After 240 hours in a 0.5 M NaCl solution, the corrosion rates of CuAlNiMn decreased from 0.144 mm/yr. to 0.087 mm/yr. while CuAlNiMnLa from 0.096 mm/yr. to 0.067 mm/yr. Additionally, after 240 hours of exposure to 1.0 M NaCl solution, the corrosion rates of CuAlNiMn decreased from 0.144 mm/yr. to 0.096 mm/yr., while CuAlNiMnLa decreased from 0.096 mm/yr. to 0.077 mm/yr.
- The micro-addition of lanthanum considerably enhanced the corrosion behavior, mechanical, and physical properties of the CuAlNiMn alloy.

Acknowledgments

The authors express their gratitude to Landmark University for aiding and fostering an environment that allowed them to begin the experimental work.

References

[1] Kanayo Alaneme K, Adebayo Ogunsanya O, Abiodun Kareem S. On The Mechanical Properties and Damping Behaviour of Thermally Aged Unmodified And Ni Modified Cu-Zn-Al Shape Memory Alloys. Vol. 58, Journal of Chemical Technology and Metallurgy. 2023. https://doi.org/10.59957/jctm.v58i6.158

[2] Anzel I, Lojen G, Ivanić I, Kosec B, Gojic M, Kòuh S, et al. Microstructural and phase analysis of CuAlNi shape-memory alloy after continuous casting. Materials and Technology [Internet]. 2013;47(2):149-52.

[3] Malinin VG, Malinina NA, Malinin G V, Malukhina OA. Development of methods of structural-analytical mesomechanics that take into account the statistical properties of martensitic transformations in materials with shape memory effect. IOP Conf Ser Mater Sci Eng. 2018;441(1). https://doi.org/10.1088/1757-899X/441/1/012030

[4] Najah Saud Al-Humairi S. Cu-Based Shape Memory Alloys: Modified Structures and Their Related Properties. In: Basheer Al-Naib U, Vikraman D, Karuppasamy K, editors. Recent Advancements in the Metallurgical Engineering and Electrodeposition [Internet]. IntechOpen; 2020. https://doi.org/10.5772/intechopen.86193

[5] Muntasir Billah AHM, Rahman J, Zhang Q. Shape memory alloys (SMAs) for resilient bridges: A state-of-the-art review. Structures. 2022 Mar 1;37:514-27. https://doi.org/10.1016/j.istruc.2022.01.034

[6] Mohamed OA, Masood SH, Xu W. Nickel-titanium shape memory alloys made by selective laser melting: a review on process optimisation. Adv Manuf. 2022 Mar 1;10(1):24-58. https://doi.org/10.1007/s40436-021-00376-9

[7] Agrawal A, Dube RK. Methods of fabricating Cu-Al-Ni shape memory alloys. J Alloys Compd. 2018 Jun 25;750:235-47. https://doi.org/10.1016/j.jallcom.2018.03.390

[8] Abolhasani D, Han SW, VanTyne CJ, Kang N, Moon YH. Enhancing the shape memory effect of Cu-Al-Ni alloys via partial reinforcement by alumina through selective laser melting. Journal of Materials Research and Technology. 2021 Nov 1;15:4032-47. https://doi.org/10.1016/j.jmrt.2021.10.040

[9] Mazzer EM, Da Silva MR, Gargarella P. Revisiting Cu-based shape memory alloys: Recent developments and new perspectives. J Mater Res [Internet]. 2022;37(1):162-82. https://doi.org/10.1557/s43578-021-00444-7
[10] Volkov-Husović T, Ivanić I, Kožuh S, Stevanović S, Vlahović M, Martinović S, et al. Microstructural and cavitation erosion behavior of the cualni shape memory alloy. Metals (Basel). 2021 Jul 1;11(7). https://doi.org/10.3390/met11070997
[11] Nwaeju C, Edoziuno F, Adediran A, Nnuka E, Adesina O. Structural and properties evolution of copper-nickel (Cu-Ni) alloys: a review of the effects of alloying materials. Matériaux & Techniques. 2021 Dec 21;109:204. https://doi.org/10.1051/mattech/2021022
[12] Yang S, Zhang J, Chen X, Chi M, Wang C, Liu X. Excellent superelasticity and fatigue resistance of Cu-Al-Mn-W shape memory single crystal obtained only through annealing polycrystalline cast alloy. Materials Science and Engineering: A. 2019 Feb 1;749. https://doi.org/10.1016/j.msea.2019.02.033
[13] Tian J, Zhu W, Wei Q, Wen S, Li S, Song B, et al. Process optimization, microstructures and mechanical properties of a Cu-based shape memory alloy fabricated by selective laser melting. J Alloys Compd. 2019 May 1;785. https://doi.org/10.1016/j.jallcom.2019.01.153
[14] Alaneme KK, Okotete EA, Anaele JU. Structural vibration mitigation - a concise review of the capabilities and applications of Cu and Fe based shape memory alloys in civil structures. Journal of Building Engineering. 2019;22:22-32. https://doi.org/10.1016/j.jobe.2018.11.014
[15] Alaneme K, Okotete E. Reconciling viability and cost-effective shape memory alloy options - A review of copper and iron based shape memory metallic systems. Engineering Science and Technology, an International Journal. 2016;19. https://doi.org/10.1016/j.jestch.2016.05.010
[16] Ivanić I, Gojić M, Kožuh S, Kosec B. Microstructural analysis of CuAlNiMn shape-memory alloy before and after the tensile testing. Materials and technologies [Internet]. 2014;713-8.
[17] Ivanić I, Gojić M, Anzel I, Kožuh S, Rimac M, Beganović O, et al. Microstructure and properties of casted CuAlNi and CuAlNiMn shape memory alloys. Vol. 55, Ljevarstvo: glasilo Hrvatskog udruženja za ljevarstvo. 2013. 79-85 p.
[18] Wang Z, Liu X, Xie J xin. Effects of solidification parameters on microstructure and mechanical properties of continuous columnar-grained Cu-Al-Ni alloy. Progress in Natural Science: Materials International. 2011;21:368-374-368-374. https://doi.org/10.1016/S1002-0071(12)60071-9
[19] Anzel I, Lojen G, Ivanić I, Kosec B, Gojic M, Kòuh S, et al. Microstructural and phase analysis of CuAlNi shape-memory alloy after continuous casting. Materials and Technology [Internet]. 2013;47(2):149-52.
[20] Akash K, Mani Prabu SS, Gustmann T, Jayachandran S, Pauly S, Palani IA. Enhancing the life cycle behaviour of Cu-Al-Ni shape memory alloy bimorph by Mn addition. Mater Lett. 2018 Sep 1;226:55-8. https://doi.org/10.1016/j.matlet.2018.05.008
[21] Guniputi BN, S.M. M. Effect of manganese and homogenization on the phase stability and properties of Cu-Al-Be shape memory alloys. Journal of Materials Research and Technology. 2021 Sep 1;14:1551-8. https://doi.org/10.1016/j.jmrt.2021.07.027
[22] Saud SN, Hamzah E, Abubakar T, Bakhsheshi-Rad HR, Zamri M, Tanemura M. Effects of Mn additions on the structure, mechanical properties, and corrosion behavior of Cu-Al-Ni shape memory alloys. J Mater Eng Perform. 2014 Oct 1;23(10):3620-9. https://doi.org/10.1007/s11665-014-1134-1
[23] Alaneme KK, Umar S. Mechanical behaviour and damping properties of Ni modified Cu-Zn-Al shape memory alloys. Journal of Science: Advanced Materials and Devices. 2018;3(3):371-9. https://doi.org/10.1016/j.jsamd.2018.05.002
[24] Peregrina-Barreto H, Terol-Villalobos IR, Rangel-Magdaleno JJ, Herrera-Navarro AM, Morales-Hernández LA, Manríquez-Guerrero F. Automatic grain size determination in

microstructures using image processing. Measurement. 2013;46(1):249-58. https://doi.org/10.1016/j.measurement.2012.06.012
[25] ASTM E92-23. Standard Test Methods for Vickers Hardness and Knoop Hardness of Metallic Materials. West Conshohocken, PA; 2023.
[26] ASTM E8/E8M-22. Standard Test Methods for Tension Testing of Metallic Materials. West Conshohocken, PA; 2022.
[27] Alaneme KK. Fracture toughness (K1C) evaluation for dual phase medium carbon low alloy steels using circumferential notched tensile (CNT) specimens. Materials Research. 2011;14(2):155-60. https://doi.org/10.1590/S1516-14392011005000028
[28] Edoziuno F, Adediran A, Adetunla A, Nwaeju C, Nnuka E. RSM-based optimization and predictive modelling of the gravimetric corrosion behaviour of solution-treated copper-based shape memory alloy in HCl solution. International Journal on Interactive Design and Manufacturing (IJIDeM). 2022 Dec 20. https://doi.org/10.1007/s12008-022-01163-x
[29] ASTM G31 -21. Standards: Metals Test Methods and Analytical Procedures. Philadelphia; 2021.
[30] Nnakwo KC, Mbah CN, Nnuka EE. Influence of trace additions of titanium on grain characteristics, conductivity and mechanical properties of copper-silicon-titanium alloys. Heliyon. 2019 Oct 1;5(10). https://doi.org/10.1016/j.heliyon.2019.e02471
[31] Nnakwo KC, Osakwe FO, Ugwuanyi BC, Oghenekowho PA, Okeke IU, Maduka EA. Grain characteristics, electrical conductivity, and hardness of Zn-doped Cu-3Si alloys system. SN Appl Sci. 2021 Nov 1;3(11). https://doi.org/10.1007/s42452-021-04784-1
[32] Alaneme K, Aluko A. Production and Age-Hardening Behaviour of Borax Premixed SiC reinforced Al-Mg-Si alloy Composites developed by Double Stir-Casting Technique. The West Indian Journal of Engineering. 2012;34.
[33] Ahmed RS, Abbass MK, AlKubaisy MM. Effect of Ce addition on mechanical properties and shape memory effect of Cu-14%Al-4.5%Ni shape memory alloy. Mater Today Proc [Internet]. 2020;20:452-60. https://doi.org/10.1016/j.matpr.2019.09.164
[34] Dalvand P, Raygan S, López GA, Chernenko VA. Effect of adding Ti and rare earth elements on properties of Cu-14Al-4Ni shape memory alloy. Mater Res Express [Internet]. 2019;6(11):116512. https://doi.org/10.1088/2053-1591/ab43f7
[35] Naik, S.N., Walley, S.M. The Hall-Petch and inverse Hall-Petch relations and the hardness of nanocrystalline metals. J Mater Sci 55, 2661-2681 (2020). https://doi.org/10.1007/s10853-019-04160-w
[36] Lu X, Chen F, Li W, Zheng Y. Effect of Ce addition on the microstructure and damping properties of Cu-Al-Mn shape memory alloys. J Alloys Compd [Internet]. 2009;480(2):608-11. https://doi.org/10.1016/j.jallcom.2009.01.134
[37] Song ZX, Li YD, Liu WJ, Yang HK, Cao YJ, Bi GL. Effect of la and sc co-addition on the mechanical properties and thermal conductivity of as-cast al-4.8% cu alloys. Metals (Basel). 2021 Nov 1;11(11). https://doi.org/10.3390/met11111866
[38] Pakdel A, Farhangi H, Emamy M. Effect of Extrusion Process on Ductility and Fracture Behavior of SiCp/Aluminum-Alloy Composites. In: Proceedings of 8th International Fracture Conference, Istanbul, Türkiye [Internet]. 2007. http://www.endil.yildiz.edu.tr/proceedings/50.pdf
[39] Alaneme KK, Sulaimon AA, Olubambi PA. Mechanical and corrosion behaviour of iron modified Cu-Zn-Al alloys. Acta Metallurgica Slovaca. 2013;19(4):292-301. https://doi.org/10.12776/ams.v19i4.184
[40] Bhattacharya S, Bhuniya A, Banerjee MK. Influence of minor additions on characteristics of Cu–Al–Ni alloy. mats sci tech. 1993 Aug 1;9(8):654-8. https://doi.org/10.1179/026708393790172358
[41] Basak Deepjyoti. Investigation of Cu based shape memory alloy as a reinforcement for metal matrix composite. 2018.

[42] Alaneme KK, Ojomo AM, Bodunrin MO. Structural analysis, mechanical and damping behaviour of Al-Zn based composites reinforced with Cu and SiC particles. Manufacturing Rev. 2022;9:5. https://doi.org/10.1051/mfreview/2022005

[43] Aliyu SJ, Adekanye TA, Adediran AA, Ikubanni PP, Ogundipe OL. A review on the effect of Rare Metals additions on the mechanical and damping properties of CuAlNi shape memory alloys. In: 2024 International Conference on Science, Engineering and Business for Driving Sustainable Development Goals (SEB4SDG). IEEE; 2024. p. 1-6. https://doi.org/10.1109/SEB4SDG60871.2024.10629969

[44] Adekanye TA, Aliyu SJ, Adediran AA, Ujunwa D, Ochimana J, Isadare B, et al. A review of CuAlNiMn shape memory alloy modified with rare earth metals. In: 2024 International Conference on Science, Engineering and Business for Driving Sustainable Development Goals (SEB4SDG). IEEE; 2024. p. 1-5. https://doi.org/10.1109/SEB4SDG60871.2024.10629987

[45] Saud SN, Hamzah E, Abubakar T, Ibrahim MK, Bahador A. Effect of a fourth alloying element on the microstructure and mechanical properties of Cu-Al-Ni shape memory alloys. J Mater Res [Internet]. 2015;30(14):2258-69. https://doi.org/10.1557/jmr.2015.196

[46] Yang L, Jiang X, Sun H, Shao Z, Fang Y, Shu R. Effect of Ta addition on microstructures, mechanical and damping properties of Cu-Al-Mn-Ti alloy. Journal of Materials Research and Technology. 2021 Nov;15:3825-35. https://doi.org/10.1016/j.jmrt.2021.10.031

[47] Ahmed Adnan RS, Abbass MK, AlKubaisy MM. Effect of Ce addition on mechanical properties and shape memory effect of Cu-14%Al-4.5%Ni shape memory alloy. Materials Today: Proceedings. 2020;20:452-60. https://doi.org/10.1016/j.matpr.2019.09.164

[48] Yang J, Wang QZ, Yin FX, Cui CX, Ji PG, Li B. Effects of grain refinement on the structure and properties of a CuAlMn shape memory alloy. Materials Science and Engineering A. 2016 May 1;664:215-20. https://doi.org/10.1016/j.msea.2016.04.009

[49] Lu X, Chen F, Li W, Zheng Y. Effect of Ce addition on the microstructure and damping properties of Cu-Al-Mn shape memory alloys. J Alloys Compd [Internet]. 2009;480(2):608-11. https://doi.org/10.1016/j.jallcom.2009.01.134

[50] Saud SN, Hamzah E, Bakhsheshi-Rad HR, Abubakar T. Effect of Ta additions on the microstructure, damping, and shape memory behaviour of prealloyed Cu-Al-Ni shape memory alloys. Scanning [Internet]. 2017;2017:1-13. https://doi.org/10.1155/2017/1789454